flow, varies between a few and ten %, depending on axial and radial station.

Entrainment data, on a quantitative basis, are not available for the aforementioned a. However, qualitative evidence shows that substantial entrainment could be taking place. Fractionally, it could be well above 10%, especially since the propellant flow rates are lower in this case. Nevertheless, it is important to note that copious entrainment could falsify the experimental evidence, only when such evidence indicates good coupling. If, as the case is here, the experimental evidence indicates poor coupling, in spite of the fact that environmental gas might enter copiously into the acceleration region, then the said coupling could not become any stronger in the absence of entrainment.

References

[1] Malliaris, A. and Libby, D. R., "Velocities of Neutral and Ionic Species in an MPD Flow," AIAA Paper 69-109, New York, 1969.

[2] Kogelschatz, U., "Doppler Shift Measurements of Axial and Rotational Velocities in an MPD Arc," *AIAA Journal*, Vol. 8, No. 1, Jan. 1970, pp. 150–154.

[3] Kruelle, G., "Characteristics and Local Analysis of MPD Thrustor Operation," AIAA Paper 67-672, Colorado Springs, Colo., 1967.

[4] Bohn, W., private communication, spring 1969, Institute of Plasmadynamics, Stuttgart, West Germany.

[5] Sovie, R. and Connolly, D., "A Study of the Axial Velocities in an Ammonia MPD Thrustor," *AIAA Journal*, Vol. 7, No. 4, April 1969, pp. 723–725.

[6] Connolly, D. and Sovie, R., "Effect of Background Pressure Magnetoplasmodynamic Thrustor Operation," *Journal of Spacecraft and Rockets*, Vol. 7, No. 3, March 1970, pp. 255–258.

[7] Malliaris, A., "Oscillations in an MPD Accelerator," *AIAA Journal*, Vol. 6, No. 8, Aug. 1968, pp. 1575–1577.

[8] Malliaris, A., "Plasma Acceleration in an Electrical Discharge by the Self-Induced Magnetic Field," *Journal of Applied Physics*, Vol. 38, No. 9, Aug. 1967, pp. 3611–3619.

[9] Malliaris, A., "Interaction of an Electrical Discharge with its Self-Induced Magnetic Field in the Presence of Gas Flow," 67-0007, Jan. 1967, Aerospace Research Labs., Wright-Patterson Air Force Base, Ohio.

[10] Powers, W., "Measurements of the Current Density Distribution in the Exhaust of an MPD Arcjet," *AIAA Journal*, Vol. 5, No. 3, March 1967, pp. 545–550.

[11] Yos, J., "Theoretical and Experimental Studies of High Temperature Gas Transport Properties," TR RAD-TR-65-7, May 1965, Avco Corp., Wilmington, Mass.

[12] Malliaris, A. and Libby, D. R., "An Investigation of MPD Accelerators," TR 70-0011, Jan. 1970, Aerospace Research Labs., Wright-Patterson Air Force Base, Ohio.

JANUARY 1971 AIAA JOURNAL VOL. 9, NO. 1

Acceleration Patterns in Quasi-Steady MPD Arcs

ROBERT G. JAHN,* KENN E. CLARK,† RONALD C. OBERTH,‡ AND PETER J. TURCHI§
Princeton University, Princeton, N. J.

Argon exhaust velocities of the order of 25,000 m/sec are observed in a quasi-steady, self-field MPD accelerator operated at 17,500 amp. The variation of measured exhaust velocity with input mass flow indicates a preferred or "matched" mass flow, at which the observed velocity substantially exceeds both the Alfvén critical speed and that computed from the electromagnetic thrust relation. Although the measured velocity corresponds roughly to the total electrode voltage, an electrostatic ion acceleration mechanism is not supported by detailed maps of the potential contours within the arc chamber. Specifically, it is found that the bulk of the arc voltage gradient, exclusive of the electrode falls, occurs within two diameters of the cathode, and is normal to it. The remainder of the arc chamber, and all of the downstream plasma is nearly equipotential, at a value close to anode sheath potential. Anode fall voltage varies inversely with local current density, implying substantially lower anode losses at higher power arc operation. Bow shocks from small obstacles placed in the exhaust stream indicate supersonic, but not hypersonic flow.

I. Introduction

QUASI-STEADY plasma propulsion involves the operation of self-field, electromagnetic thrusters in repetitive high-power pulses of sufficient duration that steady acceleration processes prevail over most of the pulse, but at repetition rates commensurate with available space power supplies. Principal attractions of this concept are the combination of arc operation in regimes of high thermal efficiency and dynamic stability with tolerable heat transfer and mean power demands, and the opportunity for variable thrust and mean power consumption without compromise in specific impulse or thruster efficiency, both accomplished via simple duty-cycle adjustment. Possible disadvantages concern the more complex power-conditioning and propellant injection implicit in systems of this type, compared to those using completely steady thrusters. Success of the concept thus hinges on coordinated efforts to minimize these system penalties through sophisticated design and technological improvements, and to exploit the advantages of high-power accelerator operation to the extent that the residual system disadvantages are more than counterbalanced. This paper attempts to contribute to the latter task by identifying some of the operating characteristics and interior physical processes of one particular quasi-steady accelerator.

Presented as Paper 70-165 at the AIAA 8th Aerospace Sciences Meeting, New York, January 19–21, 1970; submitted February 24, 1970; revision received July 16, 1970. The authors wish to express their gratitude to M. Boyle, J. Cory, A. Casini, and D. Tregurtha for their assistance in performing the experiments and interpreting the data. This work supported by NASA Grant NGL 31-001-005.

* Professor of Aerospace Sciences, Guggenheim Aerospace Propulsion Laboratories. Associate Fellow AIAA.

† Research Staff Member, Guggenheim Aerospace Propulsion Laboratories. Member AIAA.

‡ Graduate Student, Guggenheim Aerospace Propulsion Laboratories.

§ Graduate Student, Guggenheim Aerospace Propulsion Laboratories. Student Member AIAA.

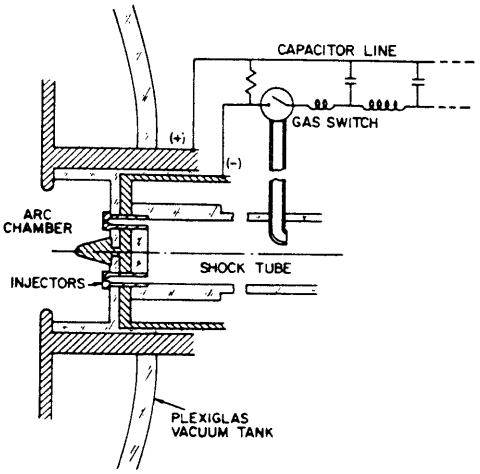

Fig. 1 Quasi-steady MPD accelerator.

The quasi-steady concept originally emerged from certain basic studies of single-pulse accelerators which indicated that essentially steady arc operation can be achieved some tens of microseconds after ignition, and that the attendant requirements on gas flow injection and stabilization can be met on a similar time scale, over a range of arc powers from hundreds of kilowatts to hundreds of megawatts.[1,2] Subsequent studies focused these techniques on a particular coaxial accelerator which closely replicated the conventional magnetoplasmadynamic (MPD) arc configuration, but on a scale one order of magnitude larger, which permitted a variety of detailed interior diagnostics including photographic observations and mapping of arc current density distributions.[3-5]

The experiments described in this paper are performed in this same accelerator, shown schematically and in photograph in Figs. 1 and 2. Briefly, the apparatus consists of a cylindrical discharge chamber with a $\frac{3}{4}$-in.-diam conical tungsten cathode and an aluminum anode with 4-in.-diam orifice driven by a 130 μfd $\times$ 10kv capacitor line which can be arranged to provide a variety of rectangular current pulses ranging from 4000 amp $\times$ 600 μsec to 140,000 amp $\times$ 20 μsec. Argon propellant gas is injected through six calibrated orifices in the arc chamber end plate from a high-pressure reservoir abruptly established by the end wall stagnation of the flow in a simple shock tube. An adjustable bleed line from the same shock tube triggers the discharge circuit switch, thereby controlling the correlation of the mass flow pattern with the arc current profile, a feature found to be essential to proper accelerator performance.[4]

II. Velocity Measurements

In the absence of direct thrust measurements, which are not possible with this particular facility, the most instructive indication of accelerator performance is the exhaust velocity pattern. Direct experimental determination of the velocity field in the exhaust plume cannot be accomplished by any classical gasdynamic techniques because of the low density, high-temperature nonequilibrium state of the flow. The

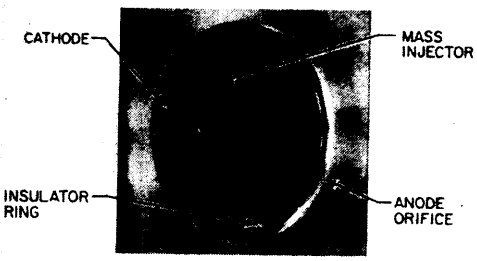

Fig. 2 View of accelerator chamber.

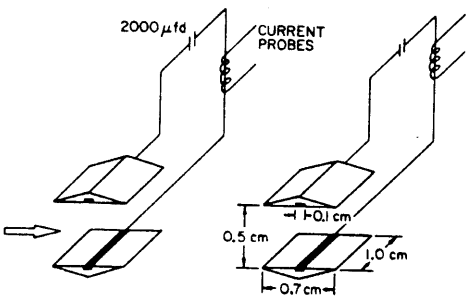

Fig. 3 Time of flight probe.

rather tedious Doppler shift methods which have provided isolated data points in a few steady MPD arcs,[6-8] fail here for lack of sufficient integrated intensity in the shifted lines. Gridded electrostatic ion energy analyzers have proven useful in certain lower power accelerators,[9-11] but in this device the high exhaust plume plasma density forces an unreasonably large expansion of any collected sample before the biasing grids can function properly. One rather simple method for velocity probing that has proven serviceable in this facility, however, involves the use of displaced pairs of biased double electrostatic probes. Passage of local fluctuations in plasma number density, convected on the exhaust stream, are recorded by a biased double probe as a fluctuation in the ion saturation current. Thus, two of these probes, separated a known distance, yield a velocity through the time of flight of these perturbations.

A schematic of such a probe arrangement, which is a modification of an earlier concept by Boyle,[12] is shown in Fig. 3. Each sensor is a 1.0 $\times$ 0.1cm copper surface mounted flush in a small nylon airfoil to keep flow disturbance to a minimum. The two probe circuits are individually biased to 10v via 2000 μfd capacitors, and their currents, as sensed by Tektronix P6021 probes, are recorded on a dual-beam oscilloscope. The complete probe assembly can be moved in the $r - z$ plane on a suitable carriage, and its axis can be inclined with respect to the accelerator centerline to establish the prevailing flow direction.

Figure 4a displays typical probe records obtained on the centerline 23.5cm downstream of the anode face, for a 17.5ka $\times$ 150 μsec driving-current pulse and a mass flow rate of 5.9 g/sec. The large initial peaks on these traces are associated with the initial starting transient of the accelerator, and the relatively long following plateaus with the quasi-steady acceleration phase. The velocity of the latter is measured by expanding a small segment of these traces on a second oscilloscope, as shown in Fig. 4b, and measuring the time displacement between characteristic features of the two probe responses.

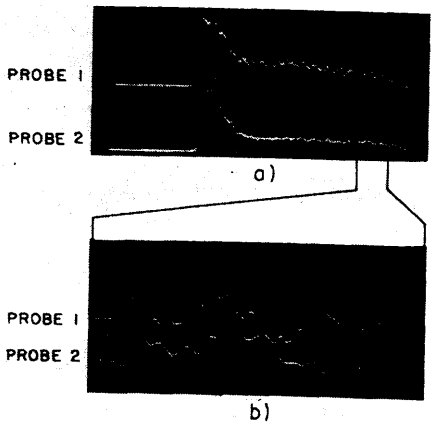

Fig. 4 Response of biased double probes; J = 17.5 ka, $\dot{m}$ = 5.9 g/sec, z = 23.5 cm, r = 0, probe spacing = 1.9 cm: a) 20 μsec/div.; b) 2 μsec/div.

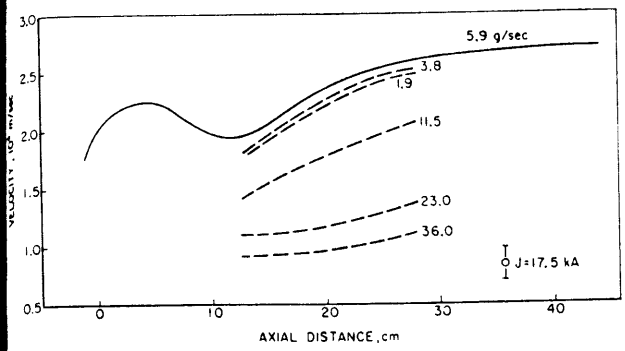

Fig. 5 Centerline velocity development for various mass flows; J = 17.5 ka.

The development of the fluctuation velocity along the thruster centerline is shown in Fig. 5 for the same operating conditions. These data indicate that the plasma leaves the anode orifice with a velocity of about 2×10^4 m/s and continues to accelerate to 2.7×10^4 m/s 30cm downstream, a value approximately twice that calculated from the electromagnetic thrust relation:[13]

$$T = (\mu J^2/4\pi)[\ln(r_a/r_c) + \tfrac{3}{4}] = \dot{m}v \qquad (1)$$

where J denotes the arc current, $\dot{m}$ the mass flow, and r_a/r_c the ratio of effective anode to cathode radii. Part of this discrepancy can be assigned to the radial nonuniformity of the velocity pattern. The radial profiles at three axial stations are shown in Fig. 6. The profile is seen to be rather steep at the 2.5cm location, but to spread rapidly to a more uniform profile at the downstream positions. From these profiles, and from estimates of particle densities derived from the magnitudes of the probe current, a mass-averaged mean velocity is calculated to be about 2.2×10^4 m/sec, a value still substantially in excess of that derived from Eq. (1). The missing increment of thrust is tentatively assigned to aerodynamic or electrothermal sources not included in the electromagnetic model.

The experimentally observed velocities are also far in excess of the so-called Alfvén critical speed[14-16]—8.7×10^3 m/s for argon—which has been proposed by some as a fundamental limit for MPD accelerators, at least those in the low power, external field category.[17,18] The physical basis for applicability of this limiting criterion to MPD accelerators is obscure, particularly in the high-power, self-field cases, and it is reassuring to observe downstream velocities a factor of three higher than this limit, in contrast to the empirical experience with external field arcs.

A principal concern of such velocity measurements derived from time of flight of plasma fluctuations is that a wave propagation component may be superimposed on the true convective velocity of the flow. For the particular environment downstream of the accelerator, the only relevant wave system would be the so-called ion acoustic mode, an electrostatically coupled longitudinal oscillation which propagates disturbances at a hybrid velocity determined by both ion and electron temperatures.[19] Using reasonable estimates of ion and electron temperature, this ion acoustic wave speed is approximately 6×10^3 m/s. Thus, even if the measured velocities are in fact the combined streaming and wave velocities, the streaming component must be at least 75% of the measured values, still well above the critical speed.

The exhaust velocity fields have also been surveyed at various other arc operating conditions. Figure 5 displays the development of centerline velocities for several different argon mass flow rates at the same arc current, 17,500 amp. Note that the data for mass flows less than the nominal value of 5.9 g/sec are indistinguishable from the 5.9 g/sec behavior; mass flows in excess of the nominal rate, in contrast, show a monatomic decrease in velocity with mass flow. The latter

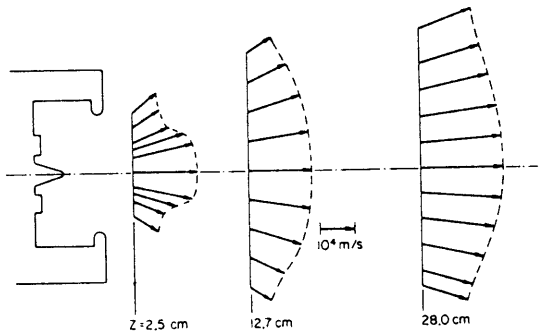

Fig. 6 Velocity pattern in accelerator exhaust; J = 17.5 ka, $\dot{m}$ = 5.9 g/sec.

behavior is qualitatively commensurate with the basic electromagnetic thrust relation Eq. (1); the former suggests that the arc has attained some limiting exhaust velocity, and is ingesting spurious mass from its electrodes, insulator, or previously ejected plasma, a familiar effect in MPD operation under "starvation" mass flow conditions.[20,21] A cross plot of such data at a given downstream location (Fig. 7) thus defines a particular mass flow, in this case about 7.5 g/sec, which has physical significance as that value at which the accelerator attains maximum exhaust velocity without spurious mass entrainment. Curiously, this value is found to coincide with the matched mass flows indicated by various other experimental and analytical criteria. For example, it is at this mass flow that the fraction of input power delivered to streamwise plasma acceleration appears to maximize.[4] Also, very recent experiments on anode processes indicate that this is just the minimum mass flow at which the full anode current can be carried by random electron flux from a surrounding equipotential plasma.[22,23] On a totally different basis, complete conversion of a 7.5 g/sec argon flow into a single-ion current, which would be appropriate to an electrostatic model of the accelerator,[24] yields a value of 18,000 amp. Further in this electrostatic vein, the observed electrode voltage at the matched condition, 150 v, corresponds almost perfectly to the kinetic energy of a single argon ion at the observed exhaust velocity.

III. Potential Patterns

The correlations of the exhaust particle kinetic energy with the discharge terminal voltage, and of the mass flow with the arc current, suggest that electrostatic processes might play a large role in the acceleration mechanism within the arc. To explore this possibility, maps of floating potential throughout the accelerator were prepared for a representative selection of operating conditions, by point-by-point probing of the discharge with a variety of electrostatic sensors. Although the results of these studies clearly negate any simple electrostatic model of the acceleration process, they provide several

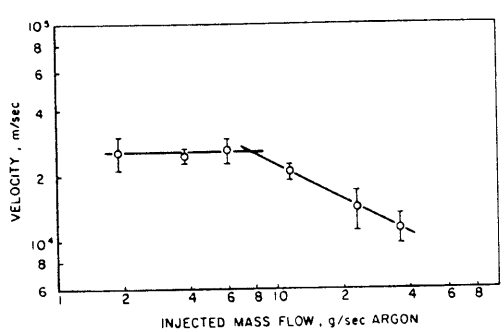

Fig. 7 Exhaust velocity dependence on mass flow rate; J = 17.5 ka, z = 28 cm.

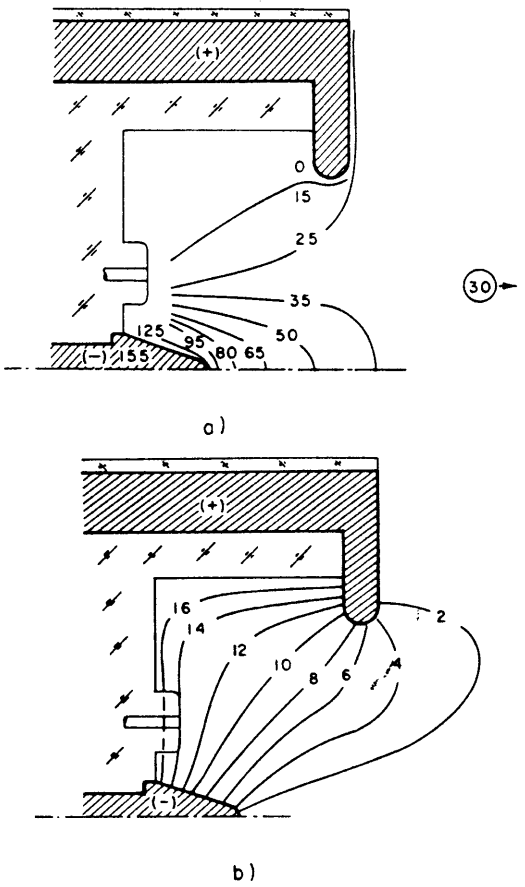

Fig. 8 Potential and current distributions in arc chamber, J = 17.5 ka, $\dot{m}$ = 5.9 g/sec: a) floating potential (negative volts, relative to anode); b) enclosed current (numbers denote total arc current downstream of contour in ka).

other valuable elements of information on the structure of the high-current discharges, particularly in connection with processes near the two electrodes.

The probes used for these measurements had three configurations of exposed surface: 1) $\frac{1}{16}$-in.-diam × $\frac{1}{16}$-in. high cone; 2) $\frac{1}{16}$-in.-diam flat disk; 3) $\frac{1}{16}$-in.-diam hemisphere. In most cases the probes were inserted axially upstream into the discharge; in a few cases the probes were inserted radially. Some probes were bent to allow access to regions behind the anode lip. All leads to the probe sensing surfaces were coaxially shielded, and the signals were presented to the oscilloscope via a Tektronix Model 6013A voltage probe of 10^8 Ω impedance.

Figure 8a displays the pattern of floating potential derived from such measurements. Interpretation of this pattern is aided by reference to the known distribution of arc current density, obtained in an earlier study,[3,4] replotted for convenience in Fig. 8b. Correction of the floating potential contours to true plasma potentials can be imposed by standard methods,[25,26] once the prevailing values of electron temperature and density, ion temperature and streaming energy are specified. In the situation at hand, the result is to displace the floating potential values some 4 to 7 v toward anode potential, depending on the location, so that the raw data are an adequate indication of the plasma potential variations.

From Fig. 8a, several significant features of the potential distribution may be identified:

1) Downstream potential differs by only 30 v (25 v if correction to plasma potential is applied) from anode potential, and by only 15 v from the region of gas injection. This is an order of magnitude lower than the observed ion kinetic energy in the exhaust stream, and hence voids any simple collisionless electrostatic acceleration model.

2) Anode fall voltage is less than 15 v (10 v) over the upstream lip of the anode where current density is a maximum (see Fig. 8b), and rises to somewhat higher value on the downstream face where current density is lower. The dependence of anode fall on current density and the implications for anode losses are discussed below.

3) The bulk of the potential drop occurs within two diameters of the cathode and is normal to it. Note that this intense field region is directed so as to decelerate ions attempting to flow downstream, hence cannot aid in a direct electrostatic acceleration process. The significance of this cathode "envelope" region is also discussed below.

4) The gas upstream of the line connecting the injector ports with the anode lip is separated from the downstream flow by about 15 v, which is roughly the ionization potential of argon. This may be coincidental, or it may reflect the ionization process functioning on the cold incoming gas.

5) Other than the regions of anode fall, cathode envelope, and ionization belt just described, the remainder of the field is essentially equipotential, indicating that the bulk of the energy input to the gas occurs in relatively small regions of the arc, most notably in the cathode envelope.

Although the hypothesis of electrostatic acceleration originally motivating the potential measurements is immediately negated by the character of the profiles, the other aspects of the patterns identified in items 2–5 above speak significantly to various features of the arc operation, and bear further discussion. For example, the observed low anode fall, and its decrease with increasing local current density, have major implications for overall efficiency of the accelerator. Steady-flow devices operating in much lower power ranges are known to dissipate large portions of their input power—in some cases 40% or more—in heating of the anode. This dissipation is clearly related to the anode fall established by the arc, and any empirical means for reducing the fall voltage should be reflected in higher overall performance. Figure 9 is a composite graph of measured anode falls at various points along the anode surface versus the current density at the same points, for three different total arc currents and matched mass flows. These data suggest a common functional dependence of anode fall on surface current density which is essentially reciprocal in the form $V_a \approx 1.5 \times 10^7/j_a$ (v/amp/m²). This in turn implies a power flux to the anode which is largely independent of the total arc current, and hence the fractional anode loss should decrease significantly with increase in total arc power.

If the arc is operated in conditions of mass starvation or mass overfeed, as defined in Section II, the character of the potential profiles changes substantially, and identification of the true anode fall becomes somewhat ambiguous. For example, Fig. 10a displays the floating potential map for the starved condition J = 17,500 amp $\dot{m}$ = 1.2 g/sec. Note the following changes from the matched condition of the same current (Fig. 8a): a) the total arc voltage has increased by 40%; b) the downstream potential has increased by a factor of 3.5; and c) there is now an envelope of potential gradient

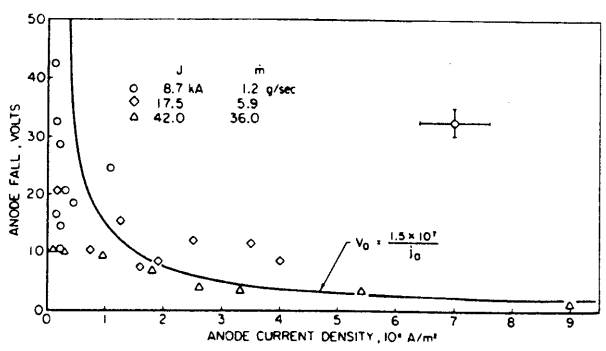

Fig. 9 Anode fall variation with local current density.

extending outward from the anode, as well as from the cathode. It is not clear whether this anode envelope is a functional part of the acceleration process, or whether it is simply a very large anode sheath necessitated by the difficult conduction conditions prevailing in the low-density environment. If ion production in the anode sheath is an essential part of the conduction process, the dimensions of the sheath would need to grow as the density dropped. In turn, if all of the power deposited in this large sheath were delivered to the anode, the fractional anode loss in this condition would be quite high.

For comparison, Fig. 10b shows the potential pattern for arc operation at the same current, but with an excessive mass flow of 36 g/sec. Here the total voltage, downstream potential, and anode envelope have all decreased, but in such proportion that the fractional anode fall power is again somewhat higher than for the matched case. The effects of mass starvation and overfeed on the potential patterns can equally well be demonstrated by fixing the mass flow and varying the arc current above and below the matched value.[27]

Returning to the nominal case of Fig. 8a, we next consider the cathode envelope region which dominates the entire potential pattern. Exclusive of the cathode fall, some two-thirds of the arc voltage is dropped across this region, and in view of the high-current densities prevailing here, it must be presumed that this zone is primarily responsible for the high exhaust velocities found downstream. Beyond this suspicion, however, no detailed model of the acceleration process is apparent. As previously remarked, the prevailing electric field accelerates positive ions inward, rather than outward. Comparison with the current profiles of Fig. 8b indicates that total current conduction in this region is largely scalar, even though electron Hall parameters greater than one can reasonably be expected near the cathode shoulder. In some portions of the envelope the electric field could reflect a large $\mathbf{u} \times \mathbf{B}$ or motional emf component, but in others, such as near the inlet orifice and along the axis, this component must be small, leaving mainly a resistive component. This in turn implies substantial ohmic heating, and possible electrothermal contributions to the overall acceleration process.

In this connection it should be noted that over most of the cathode envelope the self-magnetic body forces have large components directed radially inward which must act to compress the plasma along the axis. Thus, it may be that downstream of the cathode tip there exists a region of very hot gas, constrained by the magnetic field and heated by the electron stream which has fallen through the envelope, somewhat akin to the dense plasma focus seen in certain thermonuclear injectors.[28] Subsequent expansion of this hot gas in the magnetic nozzle may then provide a significant component of the observed exhaust kinetic energy.

IV. Mach Number Observations

Visual evidence that the plasma flow is supersonic is provided by photographs of the bow shock waves formed on small wedges inserted along the centerline. Figure 11 shows a typical photograph of a 30° half-angle wedge, 3.8cm downstream of the anode for the 17.5ka, 5.9 g/sec operating condition. The photograph was taken from the side of the accelerator (flow from left to right) through a 5 μsec Kerr-cell shutter delayed by an oscilloscope until the quasi-steady acceleration phase was well developed.

Table 1 Dependence of indicated Mach number on wedge angle and specific heat ratio

δ	θ	$M_{1.3}$	$M_{1.67}$
10°	31.5°	2.5	2.6
20°	37.5°	3.0	3.7
30°	43.0°	4.2	...
40°	51.0°	8.6	...

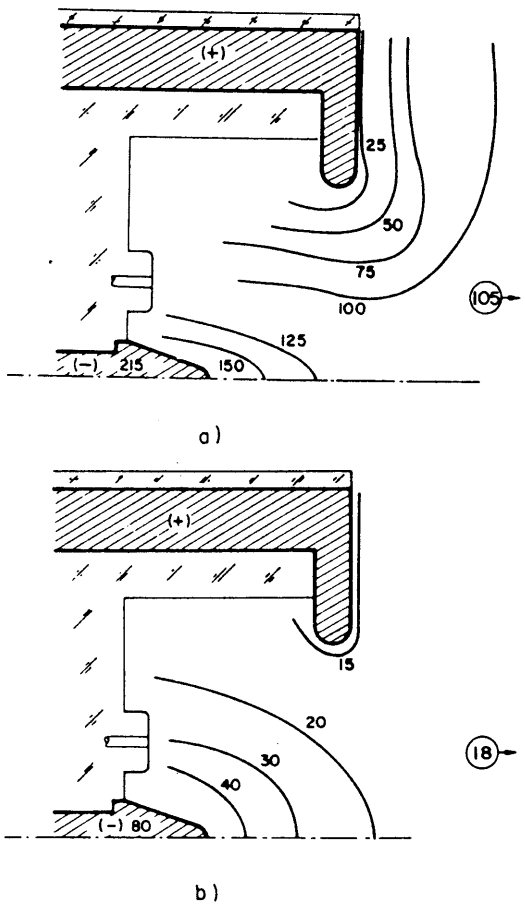

Fig. 10 Effect of mass flow on floating potential patterns, J = 17.5 ka: a) $\dot{m}$ = 1.2 g/sec (starved); b) $\dot{m}$ = 36.0 g/sec (overfed).

Deduction of Mach number from the bow shock angles requires knowledge of the effective ratio of specific heats, γ, for the plasma passing through the shocks.[29] Although this quantity could lie anywhere in the range between 1.3 and 1.67, depending on the state of equilibrium of the flow, it should be possible in principle to extract both Mach number and γ information from simultaneous consideration of data from several different wedge angles at the same location. When such an approach is attempted, however, no self-consistent solution can be found. Even when the data are taken from two surfaces of a single wedge, inclined at an angle of attack, the simultaneous solutions yield totally unreasonable values of γ. The difficulty may alternatively be illustrated by presenting values of Mach number calculated from several different wedge half-angles, δ, and shock angles, θ, for assumed values of γ of 1.3 and 1.67 (c.f., Table 1).

The wide spread in the calculated Mach numbers, or the γ paradox mentioned in Table 1, may indicate an altering of the effective deflection angle by nonideal flow effects near the wedge surface. Specifically, the strong cooling of the flow by the surface, and possible recombination effects may yield

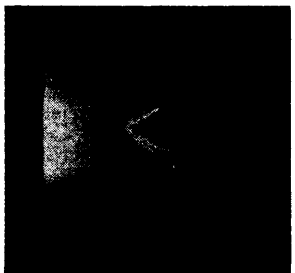

Fig. 11 30° half-angle wedge in accelerator exhaust; J = 17.5 ka, $\dot{m}$ = 5.9 g/sec, z = 3.8 cm, r = 0.

a boundary layer with a negative displacement thickness, thereby necessitating a smaller flow deflection than the nominal wedge angle. This effect should be minimized at the smaller wedge angles, since the corresponding shock waves are weaker. Thus, the 10° wedge angle data probably yields the most reliable value of Mach number, but the situation is far from satisfactory.

V. Summary

The various items of experimental data presented in this paper by no means establish a complete, self-consistent picture of the quasi-steady arc operation. They do, however, provide certain indications that the operation of self-field MPD arcs in the megawatt range differs in important respects from that at lower powers. First, the Alfvén critical velocity appears not to impose a fundamental limitation on the attainable exhaust speed; achievement of high specific impulse with heavy ions seems straightforward. Second, power loss to the anode, as indicated by the anode fall voltage, becomes proportionately less important in high-power operation; this should be reflected in higher over-all efficiency. Finally, the portion of the arc in the immediate vicinity of the cathode is indicated as the region of primary energy input, which probably controls the high-performance capability of the device.

References

[1] Eckbreth, A. C., Clark, K. E., and Jahn, R. G., "Current Pattern Stabilization in Pulsed Plasma Accelerators," *AIAA Journal*, Vol. 6, No. 11, Nov. 1968, pp. 2125–2132.

[2] Eckbreth, A. C. and Jahn, R. G., "Current Pattern and Gas Flow Stabilization in Pulsed Plasma Accelerators," *AIAA Journal*, Vol. 8, No. 1, Jan. 1970, pp. 138–143.

[3] Clark, K. E. and Jahn, R. G., "Quasi-steady Plasma Acceleration," *AIAA Journal*, Vol. 8, No. 2, Feb. 1970, pp. 216–220.

[4] Clark, K. E. and Jahn, R. G., "Quasi-steady Plasma Acceleration," NASA NGL 31-001-005, Aerospace and Mechanical Sciences Rept. 859, May 1969, Princeton Univ., Princeton, N. J.

[5] Jahn, R. G. et al., "Pulsed Electromagnetic Gas Acceleration," NASA NGL 31-001-005, Aerospace and Mechanical Sciences Rept. 634n, Jan. 1970, Princeton Univ., Princeton, N. J.

[6] Malliaris, A. C. and Libby, D. R., "Velocities of Neutral and Ionic Species in an MPD Flow," AIAA Paper 69-109, New York, 1969.

[7] Kogelschatz, U., "Doppler-shift Measurements of Axial and Rotational Velocities in an MPD Arc," *AIAA Journal*, Vol. 8, No. 1, Jan. 1970, pp. 150–154.

[8] Sovie, R. J. and Connolly, D. J., "Effect of Background Pressure on Magnetoplasmadynamic Thruster Operation," *Journal of Spacecraft and Rockets*, Vol. 7, No. 3, March 1970, pp. 255–258.

[9] Kribel, R., Eckdahl, C., and Lovberg, R., "Properties of the Rotating Spoke in an Unstable Pulsed MPD Arc," AIAA Paper 69-234, Williamsburg, Va., 1969.

[10] Ashby, D. E. T. F. et al., "Exhaust Measurements on the Plasma from a Pulsed Coaxial Gun," *AIAA Journal*, Vol. 3, No. 6, June 1965, pp. 1140–1142.

[11] Gorowitz, B., Gloersen, P., and Karras, T., "Study of Parametric Performance of a Two-stage Repetitively Pulsed Plasma Engine," GE 214-220 (summary), March 31, 1966, Space Sciences Laboratory, Missile and Space Division, General Electric Co., Philadelphia, Pa.

[12] Boyle, M. J., "Plasma Velocity Measurements with Electric Probes," B.S.E. thesis, April 1969, Princeton Univ., Princeton, N. J.

[13] Jahn, R. G., *Physics of Electric Propulsion*, McGraw-Hill, New York, 1968, pp. 240–246.

[14] Alfvén, H., "Collision Between a Nonionized Gas and a Magnetized Plasma," *Reviews of Modern Physics*, Vol. 32, Oct. 1960, pp. 710–713.

[15] Fahleson, U. V., "Experiments with Plasma Moving Through Neutral Gas," *The Physics of Fluids*, Vol. 4, No. 1, Jan. 1961, pp. 123–127.

[16] Lin, S. C., "Limiting Velocity for a Rotating Plasma," *The Physics of Fluids*, Vol. 4, No. 10, Oct. 1961, pp. 1277–1287.

[17] Patrick, R. M. and Schneiderman, A. M., "Performance Characteristics of a Magnetic Annular Arc," *AIAA Journal*, Vol. 4, No. 2, Feb. 1966, pp. 283–290.

[18] Bennett, S., John, R. R., Enos, G., and Tuchman. A., "Experimental Investigation of the MPD Arcjet," AIAA Paper 66-239, San Diego, Calif., 1966.

[19] Spitzer, L., Jr., *Physics of Fully Ionized Gases*, Interscience New York, 1962, Chap. 3.

[20] Ducati, A. C., Giannini, G. M., and Muehlberger, E., "Recent Progress in High Specific Impulse Thermo-Ionic Acceleration," AIAA Paper 65-96, New York, 1965.

[21] "Arcjet Technology Research and Development," RAD-TR-65-37, Dec. 1965, Research and Advanced Development Division, AVCO Corp., New York, N. Y.

[22] Jahn, R. G. et. al., "Pulsed Electromagnetic Gas Acceleration," NASA NGL 31-001-005, Aerospace and Mechanical Sciences Rept. 634o, July 1970, Princeton Univ., Princeton, N. J.

[23] Oberth, R. C., "Anode Phenomena in High-current Discharges," Ph.D. thesis, Dec. 1970 Princeton Univ., Princeton, N. J., forthcoming.

[24] Stratton, T. F., "High Current Steady State Coaxial Plasma Accelerators," *AIAA Journal*, Vol. 3, No. 10, Oct. 1965, pp. 1961–1963.

[25] Chen, F. F., "Electric Probes," *Plasma Diagnostic Techniques*, edited by R. H. Huddlestone and S. L. Leonard, Academic Press, New York, 1965, Chap. 4.

[26] Lam, S. H. and Greenblatt, M., "Flow of a Collisionless Plasma Over a Cone," *AIAA Journal*, Vol. 3, No. 10, Oct. 1965, pp. 1850–1854.

[27] Jahn, R. G. et al., "Acceleration Patterns in Quasi-steady MPD Arcs," AIAA Paper 70-165, New York, 1970.

[28] Mather, J. W., "Stability of the Dense Plasma Focus," *The Physics of Fluids*, Vol. 12, No. 11, Nov. 1969, pp. 2343–2347.

[29] "Equations, Tables, and Charts for Compressible Flow," Rept. 1135, 1953, NACA.